

Updated branching ratios and CP asymmetries in $D \rightarrow PV$ decays

Hui Zheng, Jia-Rui Dong and Si-Hong Zhou^{*}

School of Physical Science and Technology,

Inner Mongolia Key Laboratory of Microscale Physics and Atomic Manufacturing,

Inner Mongolia University, Hohhot 010021, China and

Center for Quantum Physics and Technologies,

School of Physical Science and Technology,

Inner Mongolia University, Hohhot 010021, China

Abstract

Motivated by extensive new high-precision experimental data, we present an updated analysis of the two-body charm decays $D \rightarrow PV$ (with $P = \pi, K, \eta^{(\prime)}$ and $V = \rho, K^*, \omega, \phi$) within the factorization-assisted topological-amplitude (FAT) approach. In the framework, flavor SU(3) symmetry breaking effect is incorporated into the topological amplitudes, allowing the nonfactorizable contributions from topological diagrams to be expressed as a minimal set of universal parameters determined through a global fit to experimental data. Thanks to the sufficient data with high precision, we are now able to quantify the nonfactorizable contribution of so-called “factorization” T diagram, which is essential for explaining the observed branching ratios. The parameters for the C , E , and A diagrams are also updated with significant improved precision, and notably, the resulting strong phases differ substantially from those in the earlier FAT analysis. We find that the C topological amplitude features substantial nonfactorizable effects in the charm sector. These refined parameters enable predictions of significantly improved accuracy, yielding branching ratios in good agreement with current data and the latest results in topological diagram approach, and the predicted direct CP asymmetries differ distinctly from previous FAT results due to updated strong phases. In several modes, the CP asymmetries are predicted to reach $\mathcal{O}(10^{-3})$, thereby making them promising observables for future high-precision experiments at LHCb, BESIII and Belle II. Predictions for unobserved decay modes, especially those with branching fractions of order $10^{-4} \sim 10^{-3}$, are also provided for forthcoming experimental tests.

^{*} corresponding author: shzhou@imu.edu.cn

I. INTRODUCTION

The charm quark, being neither heavy nor light with a mass of order 1.5 GeV, places D -meson decays at the interface of the perturbative and nonperturbative QCD. Consequently, they provide a unique testing ground for studying the corresponding decay mechanism. Furthermore, the study of CP violation in D -meson can probe for new physics. Given that CP asymmetries in the Standard Model are predicted to be of order 10^{-4} , any significant observation of CP asymmetries in hadronic charm decays would be a direct indication of physics beyond the standard model.

The theoretical description of exclusive hadronic D decay based on QCD remains an open challenge, primarily due to the intermediate scale m_c . This situation contrasts with that of nonleptonic B decays, where QCD-inspired approach like QCD factorization, perturbative QCD, and soft-collinear effective theory are successfully applicable, as they rely on a heavy quark expansion in power of $1/m_b$. For charm sector, the charm mass m_c , however, is not sufficiently heavy to allow for a sensible application of such an expansion. As a consequence, several model-independent approaches based on symmetry have been proposed. A prominent example is the topological diagram approach [1, 2], which classifies flavor-flow diagrams according to the topologies of weak interactions, incorporating all strong interaction effects. Instead of a complicated QCD analysis, this method parametrizes the corresponding topological diagram amplitudes, thereby relying on experimental measurements for the extraction of these parameters. In 2010, since a limited number of data points from Cabibbo-favored modes were available, only a subset of the topological diagram parameters could be extracted [1]. To estimate the penguin diagram contributions necessary for calculation of direct CP asymmetries, the authors subsequently employed the QCD factorization approach within the same topological framework [3]. For a systematic and global analysis of tree and penguin contributions in D decays, the FAT approach was later developed [4, 5], which successfully reproduced both the branching ratios and direct CP asymmetries, and notably resolved the long-standing puzzle of the large difference between the $D^0 \rightarrow \pi^+ \pi^-$ and $D^0 \rightarrow K^+ K^-$ branching ratios. In particular, the FAT prediction for $\Delta A_{CP}^{\text{SM}} \equiv A_{CP}(D^0 \rightarrow K^+ K^-) - A_{CP}(D^0 \rightarrow \pi^+ \pi^-) = (-0.57 \sim -1.87) \times 10^{-3}$ is consistent with the first observation of CP violation by the LHCb Collaboration in the charm sector, $\Delta A_{CP}^{\text{SM}} = (-1.54 \pm 0.29) \times 10^{-3}$ [6].

Since the 2010s, significant experimental progress has been made, with numerous new decay modes being measured and the precision of known modes continually improved, including the first observation of CP violation in the $D \rightarrow PP$ decay channels. Enabled by increasingly precise experimental data, the topological diagram approach has been continuously refined. This includes global analysis of $D \rightarrow VP$ and their CP violation in 2016 [7], 2019 [8], and 2021 [9], respectively, as well as a comprehensive update of the branching ratios for all $D \rightarrow PP, PV, VV$ decay modes in 2024 [10]. These successive studies have yielded progressively more accurate and precise predictions for the branching ratios of two-body D decays. Given this progress and ongoing accumulation of experimental results, a corresponding update of the D -meson decays within the FAT approach has become imperative.

In this work, we perform a systematic analysis of $D \rightarrow PV$ decays using the FAT approaches, incorporating the latest experimental results. The FAT framework was originally established for charm meson decays [4, 5] and subsequently generalized to B -meson decays by one of us (S.-H. Z.) and collaborators [11–13] to systematically address nonfactorizable contributions in heavy meson decays. The approach has since been successfully applied to various phenomena, including $D^0 - \bar{D}^0$ mixing [14], $K_S^0 - K_L^0$ asymmetries [15] and CP violation [16] in charm decays into neutral kaons. It has also been used to extract the CKM phase γ from charmless two-body B decays [17], while a comprehensive review of the methodology is available in [18]. More recently, the framework has been extended to both quasi-two-body B decays [19–22] and D decays [23, 24]. Building upon the topological diagram approach [1, 3], the FAT approach systematically categorizes decay amplitudes into distinct topological diagrams based on electroweak interactions, while explicitly incorporating flavor SU(3) symmetry breaking effects. Specifically, the symmetry breaking effects are implemented in the topological diagram amplitudes mainly through the factorization of form factors and decay constants, assisted by QCD factorization. The remaining nonfactorizable contributions in the topological diagram amplitudes are characterized by a minimal set of universal parameters, which are constrained through a global fit to all available experimental data. By preserving SU(3) symmetry breaking effects, the FAT approach enables a global fit using all Cabibbo-favored (CF), singly Cabibbo-suppressed (SCS), and doubly Cabibbo-suppressed (DCS) modes of $D \rightarrow PV$. In contrast, the topological diagram approach does not perform such a global analysis. Instead, it extracts the topological amplitudes exclusively from CF modes [10] and uses them to predict SCS and DCS decays. To improve agreement

with experimental SCS results, the topological diagram approach introduces SU(3) breaking corrections between SCS and CF modes via a naive factorization prescription. A further key advantage of the FAT approach lies in its unified description of penguin and tree-level contributions within a single coherent framework. This differs fundamentally from the topological diagram approach, where penguin amplitudes are typically estimated using QCD factorization, while tree-level topologies are treated diagrammatically. In the present FAT analysis, the inclusion of newer and more precise experimental data allow us to determine significantly refined nonfactorizable parameters compared to earlier FAT results [5]. These improvements translate directly into more accurate predictions for both branching ratios and direct CP asymmetries in $D \rightarrow PV$ decays, with particularly notable differences appearing in CP violation observables due to the updated determinations of strong phases.

The remainder of this paper is organized as follows. Section II introduces the theoretical framework. Numerical results and detailed discussions are presented in Sec. III. Finally, we conclude in Sec. IV.

II. FACTORIZATION AMPLITUDES FOR TOPOLOGICAL DIAGRAMS

The two-body D -meson decays proceed through the quark flavor transitions by $c \rightarrow d(s) u \bar{d}(\bar{s})$ at leading order and $c \rightarrow u q \bar{q}$ ($q = u, d, s$) at next-to-leading order in the electroweak interaction. Correspondingly, the topological diagrams consist of tree diagrams and penguin diagrams, as shown in Figs. 1 and Fig. 2, respectively. Based on the topological structures of the weak interactions, the tree diagrams are conventionally classified into four types: (a) Color-favored tree emission diagram T , (b) Color-suppressed tree emission diagram C , (c) W -exchange tree diagram E , and (d) W -annihilation tree diagram A . The penguin topologies are categorized analogously, with “tree” replaced by “penguin”, and are denoted as PT , PC , PE and PA , mirroring the tree diagram types. Unlike charmless B decays where penguin contributions dominate in certain channels such as $B \rightarrow K \pi$ [12], the corresponding penguin amplitudes in charm sector are suppressed by both the Wilson coefficients and the Cabibbo-Kobayashi-Maskawa (CKM) matrix elements. We therefore neglect these penguin contributions in the our analysis of branching fractions while retaining them for CP violation observables.

For the amplitudes corresponding to the aforementioned topological diagrams, we adopt

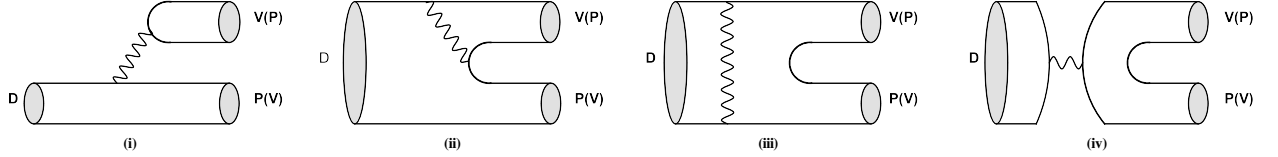


FIG. 1: Topological tree diagrams for $D \rightarrow PV$ decay with a wavy line representing the W boson: (i) color-favored tree diagram T , (ii) color-suppressed tree diagram C , (iii) W -exchange tree diagram E , and (iv) W -annihilation tree diagram A .

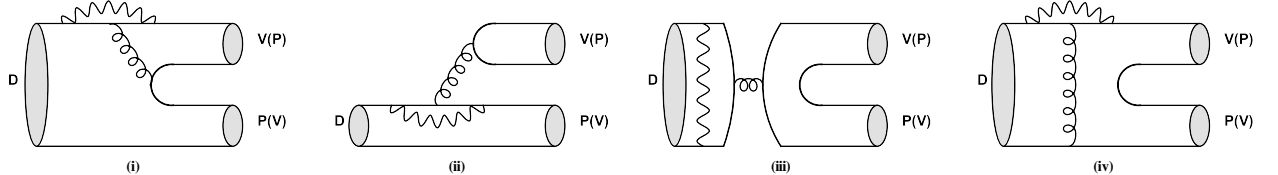


FIG. 2: Topological penguin diagrams for $D \rightarrow PV$ decay with a wavy line representing the W boson and a curly line the gluon: (i) color-favored penguin diagram PT , (ii) color-suppressed penguin diagram PC , (iii) W -exchange penguin diagram PE , and (iv) W -annihilation penguin diagram PA .

the parametrization scheme for $D \rightarrow PV$ decays as described in Ref. [5] within the FAT framework. Specifically, nonfactorizable contributions are parametrized by χ and ϕ , representing their magnitudes and associate strong phases, respectively. A key modification relative to Ref. [5] is the introduction of an additional parameter to account for nonfactorizable contributions to “factorization” T diagram. Compared to B decays, D processes exhibit significantly larger nonfactorizable contributions, even in the T diagram, owing to their lower energy release. Consequently, neglecting the nonfactorizable components of the T diagram is no longer a suitable approximation in the high-precision studies of charm decays.

The amplitudes for the various topological diagrams are given as follows, with the T diagram amplitude incorporating nonfactorizable contributions,

$$\begin{aligned}
 T_{PV}(C_{PV}) &= \sqrt{2} G_F V_{cq}^* V_{uq'} a_1(\mu) (a_2^V(\mu)) f_V m_V F_1^{DP}(m_V^2) (\varepsilon_V^* \cdot p_D), \\
 T_{VP}(C_{VP}) &= \sqrt{2} G_F V_{cq}^* V_{uq'} a_1(\mu) (a_2^P(\mu)) f_P m_V A_0^{DV}(m_P^2) (\varepsilon_V^* \cdot p_D), \\
 E_{PV,VP} &= \sqrt{2} G_F V_{cq}^* V_{uq'} C_2(\mu) \chi_{q(s)}^E e^{i\phi_{q(s)}^E} f_D m_V \frac{f_P f_V}{f_\pi f_\rho} (\varepsilon_V^* \cdot p_D), \\
 A_{PV,VP} &= \sqrt{2} G_F V_{cq}^* V_{uq'} C_1(\mu) \chi_{q(s)}^A e^{i\phi_{q(s)}^A} f_D m_V \frac{f_P f_V}{f_\pi f_\rho} (\varepsilon_V^* \cdot p_D),
 \end{aligned} \tag{1}$$

with

$$\begin{aligned} a_1(\mu) &= C_2(\mu) + C_1(\mu) \left[\frac{1}{N_C} + \chi^T \right], \\ a_2^{V(P)}(\mu) &= C_1(\mu) + C_2(\mu) \left[\frac{1}{N_C} + \chi_{V(P)}^C e^{i\phi_{V(P)}^C} \right]. \end{aligned} \quad (2)$$

The scale parameter μ , which depends on the masses of the initial and final states, is defined as

$$\mu = \sqrt{\Lambda_{\text{QCD}} m_D (1 - r_{P(V)}^2)}, \quad (3)$$

for the emission diagrams (T and C), and as

$$\mu = \sqrt{\Lambda_{\text{QCD}} m_D (1 - r_P^2)(1 - r_V^2)}, \quad (4)$$

for the annihilation diagrams (E and A). Here, $r_{P(V)} = m_{P(V)}/m_D$ denotes the mass ratio of the emitted or annihilating pseudoscalar (vector) meson from the weak vertex to the D meson. The scale evolution of the Wilson coefficients $C_{1,2}(\mu)$ for charm quark decays can be found in Ref. [4]. In Eq.(1), the subscripts PV and VP for the amplitudes T and C indicate the order of the recoiling and emitted mesons in emission diagrams, where the first particle representing the recoiling meson and the second the emitted meson. No such distinction between PV or VP configurations applies to the annihilation diagram amplitudes. The superscript $V(P)$ of the effective Wilson coefficient a_2 in Eq.(2) specifies that the emitted meson is a vector (pseudoscalar), and the same notation applies to the parameters χ and ϕ within a_2 .

We now illustrate the quantities appearing in the amplitude expressions above. The relevant CKM matrix elements involve the light-type quarks $q^{(')} = d, s$. The hadronic matrix elements are expressed in terms of the decay constants f_P and f_V of the pseudoscalar meson and vector meson, respectively, and the vector form factors F_1^{DP} and A_0^{DV} for the $D_{(s)} \rightarrow P$ and $D_{(s)} \rightarrow V$ transitions. The remaining quantities, m_V , ϵ_V^* , and p_D , correspond to the vector meson mass, its polarization vector, and the D -meson momentum, respectively. The symbols χ^T , $\chi_{V(P)}^C$, $\chi_{q(s)}^E$, and $\chi_{q(s)}^A$ represent the magnitudes of nonfactorizable contributions in the topological diagrams T , C , E and A , respectively, with associated strong phases denoted by $\phi_{V(P)}^C$, $\phi_{q(s)}^E$, and $\phi_{q(s)}^A$. The nonfactorizable contributions contain vertex corrections, hard spectator interactions involving the spectator quark of the D meson, and FSI effects from inelastic rescattering, resonance effects, etc. These unknown nonfactorizable

parameters are to be determined through a global fit to experimental data. To minimize free parameters, we retain only the relative phase of the T diagram with respect to other amplitudes, and thus do not introduce its absolute strong phase. For color-suppressed C diagram, nonfactorization contributions, such as final-state interaction and resonance effects, are dominated and differ between C_{PV} and C_{VP} amplitudes. We therefore introduce two distinct sets of parameters, χ_V^C, ϕ_V^C and χ_P^C, ϕ_P^C , corresponding to the case where the emitted meson is a vector (V) or a pseudoscalar (P) particle, respectively. For the annihilation-type E and A amplitudes, in addition to accounting for $SU(3)$ breaking effects from the decay constants of initial and final-state particles, we use subscripts q and s in the parameters $\chi_{q(s)}^E, \chi_{q(s)}^A, \phi_{q(s)}^E$, and $\phi_{q(s)}^A$ to distinguish whether the strongly produced quark pair consists of light-quarks ($u\bar{u}$ or $d\bar{d}$) or strange-quarks ($s\bar{s}$). As explained in Ref. [5], this treatment of $SU(3)$ breaking effect is more essential for accurately modeling the dynamics of E and A annihilation topologies in D decays than accounting for isospin symmetry breaking ($\chi_{P(V)}$ adopted in [1]). Another strong phase not represented in the expressions of the two annihilation amplitudes is the Glauber phase S_π , which arises from soft gluon interactions in the two-body heavy meson decays. It has been proposed that the Glauber effect plays a significant role in processes with a pion in the final state [4, 5]. Following Ref. [5], we incorporate this Glauber phase only in the E and A amplitudes, but not in the emission diagrams. The relative phase sufficiently accounts for the interference effects between the annihilation and emission processes. In total, our parametrization of $D \rightarrow PV$ decays at tree level comprises 15 free parameters: the soft scale Λ_{QCD} ; the magnitudes of the nonfactorizable amplitudes $\chi^T, \chi_{V(P)}^C, \chi_{q(s)}^E$, and $\chi_{q(s)}^A$ along with their associated strong phase $\phi_{V(P)}^C, \phi_{q(s)}^E$, and $\phi_{q(s)}^A$; and Glauber phase S_π .

As penguin type amplitudes from Fig. 2 are highly suppressed, they can be safely neglected in the analysis of branching ratios. However, these amplitudes must be retained in calculations of CP asymmetries, where interference between tree and penguin amplitudes plays a critical role. The formulas of penguin amplitudes are expected to be analogous in form to the tree amplitudes in Eq.(1), but with distinct nonfactorizable parameters, i.e. $\chi^{PT}, \chi_{V(P)}^{PC}, \chi_{q(s)}^{PE}$, and $\chi_{q(s)}^{PA}$ and their associated strong phases as implemented in Ref. [5]. In principle, these parameters should be determined from experimental data, particularly from measurements of CP asymmetries. However, neither a sufficient amount of high precision branching ratio data nor any measured CP asymmetries in two-body D decays are currently

available. We therefore adopt the approximation of using the same nonfactorizable parameters for the penguin amplitudes as those introduced for tree topologies. The treatment is well justified for the following reasons.

For PT amplitude, the factorizable contribution dominates. The matrix elements of the penguin operators $O_3 = (\bar{u}_\alpha c_\alpha)_{V-A} (\bar{d}_\beta d_\beta)_{V-A}$ $O_4 = (\bar{u}_\alpha c_\beta)_{V-A} (\bar{d}_\beta d_\alpha)_{V-A}$ are identical to those of the tree operators $O_1 = (\bar{u}_\alpha d_\alpha)_{V-A} (\bar{d}_\beta c_\beta)_{V-A}$ $O_2 = (\bar{u}_\alpha d_\beta)_{V-A} (\bar{d}_\beta c_\alpha)_{V-A}$ via the Fiertz transformation. It is therefore reasonable to adopt the same parameter χ^T to account for nonfactorizable effects in the PT amplitudes. The additional penguin operators $O_5 = (\bar{u}_\alpha c_\alpha)_{V-A} (\bar{d}_\beta d_\beta)_{V+A}$ and $O_6 = (\bar{u}_\alpha c_\beta)_{V-A} (\bar{d}_\beta d_\alpha)_{V+A}$ contribute exclusively to the penguin amplitude PT_{VP} , where the emitted particle is a pseudoscalar meson. As an approximation, we use the same parameter χ^T to characterize their nonfactorizable contributions. Their explicit forms are given by

$$\begin{aligned} PT_{PV} &= -\sqrt{2} G_F V_{cb}^* V_{ub} a_4(\mu) f_V m_V F_1^{DP}(m_V^2) (\varepsilon_V^* \cdot p_D), \\ PT_{VP} &= -\sqrt{2} G_F V_{cb}^* V_{ub} [a_4(\mu) - r_\chi a_6(\mu)] f_P m_V A_0^{DV}(m_P^2) (\varepsilon_V^* \cdot p_D) \end{aligned} \quad (5)$$

with the chiral factor $r_\chi = 2m_0^P/m_c$ and the effective Wilson coefficients

$$\begin{aligned} a_4(\mu) &= C_4(\mu) + C_3(\mu) \left[\frac{1}{N_c} + \chi^T \right], \\ a_6(\mu) &= C_6(\mu) + C_5(\mu) \left[\frac{1}{N_c} + \chi^T \right]. \end{aligned} \quad (6)$$

Since the penguin annihilation diagram PA share the same topological structure as PT and differ only in gluon interactions, it can be regarded as a power correction to PT amplitude. Its contribution is therefore absorbed into the nonfactorizable parameter of PT , specifically, through the parameter χ^T , as done in Ref. [12].

The nonfactorizable contribution of color-suppressed PC amplitude form O_4 and O_6 are found to be identical in the PQCD analyses [25]. We thus use the same parameters $\chi_{V(P)}^C$ and $\phi_{V(P)}^C$ for PC amplitude, as given below

$$\begin{aligned} PC_{PV} &= -\sqrt{2} G_F V_{cb}^* V_{ub} [a_3^V(\mu) + a_5^V(\mu)] f_V m_V F_1^{DP}(m_V^2) (\varepsilon_V^* \cdot p_D), \\ PC_{VP} &= -\sqrt{2} G_F V_{cb}^* V_{ub} [a_3^P(\mu) - a_5^P(\mu)] f_P m_V A_0^{DV}(m_P^2) (\varepsilon_V^* \cdot p_D), \end{aligned} \quad (7)$$

with the effective Wilson coefficients

$$\begin{aligned} a_3^{V(P)}(\mu) &= C_3(\mu) + C_4(\mu) \left[\frac{1}{N_c} + \chi_{V(P)}^C e^{i\phi_{V(P)}^C} \right], \\ a_5^{V(P)}(\mu) &= C_5(\mu) + C_6(\mu) \left[\frac{1}{N_c} - \chi_{V(P)}^C e^{i\phi_{V(P)}^C} \right]. \end{aligned} \quad (8)$$

For the amplitude PE , the nonfactorizable contributions from operators $O_{4,6}$ have also been analyzed in Ref. [25] and can be expressed using the same parameterization as

$$PE_{PV,VP} = -\sqrt{2} G_F V_{cb}^* V_{ub} [C_4(\mu) - C_6(\mu)] \chi_{q,s}^E e^{i\phi_{q,s}^E} f_D m_V \frac{f_P}{f_\pi} \frac{f_V}{f_\rho} (\varepsilon_V^* \cdot p_D). \quad (9)$$

In the subsequent analysis of CP violation, we also incorporate contributions from chromomagnetic penguin operators and quark-loops corrections, which influence penguin-induced CP asymmetries. Following the treatment in Ref. [26–28], these effects are absorbed into an effective redefinition of the Wilson coefficients $C_{3,4,5,6}$ and explicit expressions can also be found in Ref. [5].

III. NUMERICAL RESULTS AND DISCUSSIONS

A. Input parameters

The input parameters in the amplitudes of Eq.(1) can be classified as electroweak coefficients, short-distance physics coefficients and nonperturbative QCD parameters. The electroweak parameters, namely the CKM matrix elements, are taken from the PDG [29]. The Wilson coefficients, encoding the short-distance physics in D decays, are adopted from the Appendix of Ref. [4].

The nonperturbative QCD input include decay constants and transition form factors. The decay constants for pseudoscalar mesons and vector mesons (in units of MeV) are summarized in Table I. Those for the π , K and $D_{(s)}$ are taken from the PDG [29], while for vector mesons not yet measured experimentally, we employ the same theoretical values used in quasi-two-body decays of B -meson, assigning 5% uncertainty [21].

TABLE I: Decay constants of pseudoscalar and vector mesons.

f_π	f_K	f_D	f_{D_s}	f_ρ	f_{K^*}	f_ω	f_ϕ
130.2 ± 1.7	155.6 ± 0.4	211.9 ± 1.1	258 ± 12.5	213 ± 11	220 ± 11	192 ± 10	225 ± 11

The transition form factors for D decays, such as $D \rightarrow \pi$ and $D \rightarrow K$, have been measured by experiments including CLEO-c [30], Belle [31], and BESIII [32, 33]. For transitions lacking experimental measurements, theoretical predictions are available from a variety of

approaches, such as Lattice QCD [34], QCD sum rules [35, 36], quark models [37], the covariant light-front quark model [38–40], Improved light-cone harmonic oscillator model [41], heavy meson and chiral symmetries (HM_χT) [42], Hard-Wall AdS/QCD model [43], and 4-flavor holographic QCD [44]. In light of the discrepancies in form factor predictions from different approaches, the values adopted at zero recoil ($Q^2 = 0$) are chosen to be consistent with the current experimental and theoretical landscape. A 10 % uncertainty is consequently kept to account for the theoretical variations. The adopted values of the form factors at $Q^2 = 0$ and the associated α_i parameters from Ref. [45], are provided in Table II. Their Q^2 dependence is uniformly parameterized by the dipole form used in Ref. [4, 5, 45]

$$F_i(Q^2) = \frac{F_i(0)}{1 - \alpha_1 \frac{Q^2}{m_{\text{pole}}^2} + \alpha_2 \frac{Q^4}{m_{\text{pole}}^4}}, \quad (10)$$

where F_i stands for F_1 or A_0 . The pole mass m_{pole} takes the value m_{D^*} for $F_1^{D\pi, D\eta^{(*)}, D_s K}$, $m_{D_s^*}$ for $F_1^{DK, D_s \eta^{(*)}}$, m_D for $A_0^{D\rho, D\omega, D_s K^*}$, and m_{D_s} for $A_0^{DK^*, D_s \phi}$.

TABLE II: Form factors and dipole model parameters.

	$F_1^{D \rightarrow \pi}$	$F_1^{D \rightarrow K}$	$F_1^{D_s \rightarrow K}$	$F_1^{D \rightarrow \eta_q}$	$F_1^{D \rightarrow \eta_s}$
$F_i(0)$	0.60	0.74	0.66	0.76	0.79
α_1	1.24	1.33	1.20	1.03	1.23
α_2	0.24	0.33	0.20	0.29	0.23
	$A_0^{D \rightarrow \rho}$	$A_0^{D \rightarrow K^*}$	$A_0^{D_s \rightarrow K^*}$	$A_0^{D \rightarrow \omega}$	$A_0^{D_s \rightarrow \phi}$
$F_i(0)$	0.84	0.73	0.68	0.68	0.70
α_1	1.36	1.17	1.20	1.36	1.10
α_2	0.36	0.17	0.20	0.36	0.10

B. The updated nonfactorizable parameters

The nonfactorizable parameters of the topological tree diagram amplitudes of Eq.(1) consist of 15 free quantities: χ^T , $\chi_{V(P)}^C$, $\chi_{q(s)}^E$, and $\chi_{q(s)}^A$, along with their associated phases $\phi_{V(P)}^C$, $\phi_{q(s)}^E$, $\phi_{q(s)}^A$, and S_π (where the factor e^{iS_π} multiplies the E and A amplitudes), as well as the soft scale Λ_{QCD} [see Eqs.(3) (4)]. These unknown parameters are determined by a

global fit to 41 experimental measurements of $D \rightarrow PV$ branching ratios with significance above 3σ from PDG [29]. This dataset has higher precision and includes more data points than the 33 used in [5]. The best-fit values and their corresponding uncertainties are as follows

$$\begin{aligned}
\chi^T &= -0.29 \pm 0.01, \\
\chi_P^C &= -0.47 \pm 0.02, \quad \phi_P^C = 0.37 \pm 0.12, \\
\chi_V^C &= -0.41 \pm 0.01, \quad \phi_V^C = -0.52 \pm 0.02, \\
\chi_q^E &= 0.13 \pm 0.01, \quad \phi_q^E = 2.68 \pm 0.10, \\
\chi_s^E &= 0.24 \pm 0.01, \quad \phi_s^E = 3.52 \pm 0.07, \\
\chi_q^A &= 0.10 \pm 0.003, \quad \phi_q^A = -2.08 \pm 0.16, \\
\chi_s^A &= 0.18 \pm 0.01, \quad \phi_s^A = 2.62 \pm 0.10, \\
S_\pi &= -1.80 \pm 0.17, \quad \Lambda_{\text{QCD}} = (0.24 \pm 0.01) \text{GeV},
\end{aligned} \tag{11}$$

with $\chi^2/\text{d.o.f.} = 6.2$. These nonfactorizable parameters are determined with high precision, with the exception of the strong phase ϕ_P^C . The precision for this phase is limited due to insufficient experimental data from decay modes dominated by the C_{VP} amplitude. The nonfactorizable contribution of the T topology, χ^T , is non-negligible. The term $C_1 \chi^T$ is comparable in magnitude to its factorizable counterpart, C_1/N_C , from O_1 operator. The C amplitude parameters χ_P^C and χ_V^C show slight deviations from the values obtained early [5] (note that the labeling of χ_P^C and χ_V^C is reversed relative to Ref. [5]). The more significant discrepancies, however, arises from the the E and A topologies, which are dominated by non-factorizable dynamics. Specifically, the fitted values of $\chi_{q,s}^{E,A}$ together with the strong phases $\phi_{q,s}^{E,A}$ and the Glauber phase S_π , collectively account for these observed differences. The reason lie in the fact that the dominant T and C amplitudes were already well-determined with the prior data, whereas the subleading E and A topological amplitudes are smaller and thus require a larger set of high-precision measurements to be accurately constrained. The Λ_{QCD} obtained in this work is physically reasonable. For instance, in the $D^+ \rightarrow \bar{K}^0 \rho^+$ decay mode, the corresponding scale is $\mu = 0.61 \text{ GeV}$ (with $\Lambda_{\text{QCD}} = 0.24 \text{ GeV}$), yielding a value approximately $m_c/2$. At this scale, the Wilson coefficients for the T and C amplitudes are $a_1(\mu) = 1.45$ and $a_2^P(\mu) = -1.09 e^{i0.26}$, indicating that while the T topology dominates D decays, the C topology also features substantial nonfactorizable effects.

C. Branching Ratios

Our numerical results for the branching ratios of $D_{(s)}$ decays are collected in Tables III-V, corresponding to the CF ($V_{cs}^* V_{ud}$), SCS ($V_{cd(s)}^* V_{ud(s)}$), and DCS ($V_{cd}^* V_{us}$) modes, respectively. In our results, denoted as “Br(FAT)”, the first uncertainty is statistical, originating from the nonperturbative parameters in Eq.(11) via the χ^2 fit to the experimental data. The second and third uncertainties arise from the form factors and the decay constants, respectively. As shown in our results, the uncertainty is dominated by the contributions from the form factors. The topological diagram amplitudes $T_{PV,VP}, C_{PV,VP}, E, A$ are provided in the second columns of these tables to facilitate the analysis of branching ratio hierarchies therein. We list all available experimental data, including those with significance below 3σ , in the third column for comparing with our results. Finally, the last two columns present the latest results updated in the topological diagram approach for comparison, specifically the (F4) and (F1') corresponding to two distinct solutions derived from different fitted topological amplitude parameters [10]. Our results are consistent with the measured CF and SCS modes. Regarding DCS decays, most of them have not yet been experimentally measured, so our predictions can be tested with future data. Compared with the results from the topological diagram approach, most of our findings are in good agreement with them. The updated results in the two different theoretical approaches, especially for DCS decays, can serve as a valuable cross-check.

Among the CF modes, the decays $D^0 \rightarrow K^- \rho^+$ (with T_{PV} and E amplitudes) and $D^+ \rightarrow \bar{K}^0 \rho^+$ (with T_{PV} and C_{VP} amplitudes) exhibit the largest branching ratios, confirming their dominance by the T_{PV} topology. These largest branching ratios originate from the large Wilson coefficient $a_1(\mu)$ and sizable vector meson decay constant in T_{PV} amplitude. Although the ratio $|a_2^P/a_1| = 0.75$ might suggest comparable contributions from the T_{PV} and C_{VP} in $D^+ \rightarrow \bar{K}^0 \rho^+$, the smaller pseudoscalar meson decay constant in C_{VP} amplitude leads to a dominant T_{PV} contribution and a suppressed C_{VP} component. In contrast, for $D^+ \rightarrow \pi^+ \bar{K}^{*0}$, the T_{VP} and C_{PV} amplitudes add incoherently, yielding a branching ratio nearly one order of magnitude smaller than that of $D^+ \rightarrow \bar{K}^0 \rho^+$. In decays involving both the T and E or C and E topologies, a strong coherence cannot be established between the amplitude $T_{PV(VP)}$ and E or between $C_{PV(VP)}$ and E . This is supported by the decay $D^0 \rightarrow \pi^0 \bar{K}^{*0}$, where the ratio $E/C_{PV} = 0.18$ implies a strong suppression of the E amplitude. Therefore,

TABLE III: Branching ratios for the Cabibbo-favored $D \rightarrow PV$ decays in units of percentage. Our results (FAT) are compared with the experimental data (EXP) [29] and the updated results (F4) and (F1') from the topological diagram approach. The second column lists the corresponding topological diagram contributions, denoted by $T_{PV,VP}, C_{PV,VP}, E$ and A .

Modes	Amplitudes	Br(EXP)	Br(FAT)	Br(F4)	Br(F1')
$D^0 \rightarrow \pi^+ K^{*-}$	T_{VP}, E	5.34 ± 0.41	$6.05 \pm 0.46 \pm 0.97 \pm 0.17$	5.45 ± 0.34	5.37 ± 0.33
$D^0 \rightarrow \pi^0 \bar{K}^{*0}$	C_{PV}, E	3.74 ± 0.27	$3.33 \pm 0.30 \pm 0.58 \pm 0.34$	3.61 ± 0.18	3.70 ± 0.18
$D^0 \rightarrow \bar{K}^0 \rho^0$	C_{VP}, E	1.26 ± 0.16	$1.08 \pm 0.14 \pm 0.27 \pm 0.04$	1.25 ± 0.09	1.25 ± 0.09
$D^0 \rightarrow \bar{K}^0 \omega$	C_{VP}, E	2.22 ± 0.12	$2.06 \pm 0.16 \pm 0.31 \pm 0.08$	2.29 ± 0.11	2.29 ± 0.11
$D^0 \rightarrow \bar{K}^0 \phi$	E	0.825 ± 0.061	$0.64 \pm 0.06 \pm 0.00 \pm 0.09$	0.830 ± 0.034	0.828 ± 0.034
$D^0 \rightarrow K^- \rho^+$	T_{PV}, E	11.2 ± 0.7	$10.41 \pm 0.48 \pm 2.46 \pm 1.06$	11.4 ± 0.8	11.3 ± 0.7
$D^0 \rightarrow \eta \bar{K}^{*0}$	C_{PV}, E	1.41 ± 0.12	$0.92 \pm 0.11 \pm 0.18 \pm 0.09$	1.35 ± 0.06	1.41 ± 0.07
$D^0 \rightarrow \eta' \bar{K}^{*0}$	C_{PV}, E	≤ 0.1	$0.013 \pm 0.002 \pm 0.001 \pm 0.001$	0.0055 ± 0.0004	0.0043 ± 0.0003
$D^+ \rightarrow \pi^+ \bar{K}^{*0}$	T_{VP}, C_{PV}	1.57 ± 0.13	$1.59 \pm 0.13 \pm 0.51 \pm 0.24$	1.58 ± 0.13	1.58 ± 0.13
$D^+ \rightarrow \bar{K}^0 \rho^+$	T_{PV}, C_{VP}	12.28 ± 1.2	$10.48 \pm 1.11 \pm 4.20 \pm 1.92$		
$D_s^+ \rightarrow \pi^+ \rho^0$	A	0.020 ± 0.012	0	0.011 ± 0.003	0.011 ± 0.002
$D_s^+ \rightarrow \pi^+ \omega$	A	0.238 ± 0.015	$0.24 \pm 0.02 \pm 0.00 \pm 0.03$	0.24 ± 0.01	0.24 ± 0.01
$D_s^+ \rightarrow \pi^+ \phi$	T_{VP}	4.5 ± 0.12	$4.45 \pm 0.08 \pm 0.89 \pm 0.01$	4.49 ± 0.11	4.50 ± 0.11
$D_s^+ \rightarrow \pi^0 \rho^+$	A		0	0.012 ± 0.003	0.011 ± 0.002
$D_s^+ \rightarrow K^+ \bar{K}^{*0}$	C_{PV}, A	3.79 ± 0.09	$3.70 \pm 0.25 \pm 1.00 \pm 0.39$	3.80 ± 0.10	3.79 ± 0.09
$D_s^+ \rightarrow \bar{K}^0 K^{*+}$	C_{VP}, A	1.54 ± 0.14	$1.72 \pm 0.24 \pm 0.42 \pm 0.05$		
$D_s^+ \rightarrow \eta \rho^+$	T_{PV}, A	8.9 ± 0.8	$9.10 \pm 0.39 \pm 1.91 \pm 0.91$	9.25 ± 0.35	8.75 ± 0.31
$D_s^+ \rightarrow \eta' \rho^+$	T_{PV}, A	5.8 ± 1.5	$4.04 \pm 0.11 \pm 0.77 \pm 0.40$	3.24 ± 0.11	3.60 ± 0.11

the E diagram can be neglected to a good approximation in the processes involving both T and E , or C and E . The observed branching fraction relations in CF decays, $\text{Br}(D^0 \rightarrow K^- \rho^+) \approx 2 \text{Br}(D^0 \rightarrow \pi^+ K^{*-}) \text{Br}(D^0 \rightarrow \pi^0 \bar{K}^{*0}) \approx 3 \text{Br}(D^0 \rightarrow \bar{K}^0 \rho^0)$, and $\text{Br}(D_s^+ \rightarrow K^+ \bar{K}^{*0}) \approx 2 \text{Br}(D^0 \rightarrow \bar{K}^0 K^{*+})$ can be explained by the negligible E amplitudes and the consequent by a factor of 2–3 for modes with T_{PV} or C_{PV} amplitudes over those with T_{VP} or C_{VP} modes, owing to the much larger the decay constants of light vector mesons compared to light pseudoscalar ones. A similar hierarchy is likewise evident in SCS

TABLE IV: Same as Table III for the singly Cabibbo-suppressed $D \rightarrow PV$ decays in units of 10^{-3} .

Modes	Amplitudes	Br(EXP)	Br(FAT)	Br(F4)	Br(F1')
$D^0 \rightarrow \pi^+ \rho^-$	T_{VP}, E	5.15 ± 0.25	$4.93 \pm 0.34 \pm 0.82 \pm 0.12$	5.42 ± 0.12	5.23 ± 0.18
$D^0 \rightarrow \pi^0 \rho^0$	C_{PV}, C_{VP}, E	3.86 ± 0.23	$3.04 \pm 0.28 \pm 0.34 \pm 0.21$	2.86 ± 0.06	3.38 ± 0.10
$D^0 \rightarrow \pi^0 \omega$	C_{PV}, C_{VP}, E	0.117 ± 0.035	$0.23 \pm 0.08 \pm 0.08 \pm 0.05$	0.157 ± 0.015	0.153 ± 0.021
$D^0 \rightarrow \pi^0 \phi$	C_{PV}	1.17 ± 0.04	$1.16 \pm 0.05 \pm 0.23 \pm 0.12$	0.93 ± 0.02	0.99 ± 0.02
$D^0 \rightarrow \pi^- \rho^+$	T_{PV}, E	10.1 ± 0.4	$9.65 \pm 0.51 \pm 1.70 \pm 0.97$	10.6 ± 0.5	10.2 ± 0.6
$D^0 \rightarrow K^+ K^{*-}$	T_{VP}, E	1.65 ± 0.11	$1.30 \pm 0.10 \pm 0.34 \pm 0.06$	1.65 ± 0.04	1.55 ± 0.04
$D^0 \rightarrow K^0 \overline{K}^{*0}$	E	0.246 ± 0.048	$0.35 \pm 0.07 \pm 0.00 \pm 0.05$	0.246 ± 0.011	0.246 ± 0.021
$D^0 \rightarrow \overline{K}^0 K^{*0}$	E	0.336 ± 0.063	$0.35 \pm 0.07 \pm 0.00 \pm 0.05$	0.336 ± 0.021	0.336 ± 0.015
$D^0 \rightarrow K^- K^{*+}$	T_{PV}, E	4.56 ± 0.21	$5.01 \pm 0.21 \pm 1.17 \pm 0.51$	4.57 ± 0.22	4.56 ± 0.15
$D^0 \rightarrow \eta \rho^0$	C_{PV}, C_{VP}, E		$0.49 \pm 0.12 \pm 0.10 \pm 0.00$	0.26 ± 0.02	0.25 ± 0.02
$D^0 \rightarrow \eta \omega$	C_{PV}, C_{VP}, E	1.98 ± 0.18	$2.78 \pm 0.16 \pm 0.35 \pm 0.13$	1.71 ± 0.05	1.99 ± 0.06
$D^0 \rightarrow \eta \phi$	C_{PV}, E	0.18 ± 0.05	$0.25 \pm 0.05 \pm 0.01 \pm 0.03$	0.175 ± 0.007	0.186 ± 0.004
$D^0 \rightarrow \eta' \rho^0$	C_{PV}, C_{VP}, E		$0.24 \pm 0.01 \pm 0.03 \pm 0.01$	0.059 ± 0.002	0.059 ± 0.002
$D^0 \rightarrow \eta' \omega$	C_{PV}, C_{VP}, E		$0.02 \pm 0.00 \pm 0.00 \pm 0.00$	0.017 ± 0.001	0.009 ± 0.001
$D^+ \rightarrow \pi^+ \rho^0$	T_{VP}, C_{PV}, A	0.83 ± 0.14	$0.51 \pm 0.05 \pm 0.13 \pm 0.01$	0.55 ± 0.06	0.57 ± 0.05
$D^+ \rightarrow \pi^+ \omega$	T_{VP}, C_{PV}, A	0.28 ± 0.06	$0.28 \pm 0.10 \pm 0.19 \pm 0.05$	0.31 ± 0.05	0.88 ± 0.07
$D^+ \rightarrow \pi^+ \phi$	C_{PV}	5.7 ± 0.14	$5.91 \pm 0.22 \pm 1.18 \pm 0.59$	4.74 ± 0.10	5.03 ± 0.10
$D^+ \rightarrow \pi^0 \rho^+$	T_{PV}, C_{VP}, A		$3.20 \pm 0.28 \pm 1.18 \pm 0.55$	5.20 ± 0.33	5.25 ± 0.38
$D^+ \rightarrow K^+ \overline{K}^{*0}$	T_{VP}, A	3.71 ± 0.18	$3.91 \pm 0.20 \pm 0.94 \pm 0.12$	5.78 ± 0.15	5.26 ± 0.14
$D^+ \rightarrow \overline{K}^0 K^{*+}$	T_{PV}, A	17.3 ± 1.8	$13.98 \pm 0.42 \pm 3.12 \pm 1.41$	15.8 ± 0.5	15.6 ± 0.5
$D^+ \rightarrow \eta \rho^+$	T_{PV}, C_{VP}, A		$0.18 \pm 0.16 \pm 0.13 \pm 0.04$	0.38 ± 0.18	0.36 ± 0.19
$D^+ \rightarrow \eta' \rho^+$	T_{PV}, C_{VP}, A		$1.71 \pm 0.05 \pm 0.24 \pm 0.10$	0.97 ± 0.03	1.12 ± 0.03
$D_s^+ \rightarrow \pi^+ K^{*0}$	T_{VP}, A	2.55 ± 0.35	$2.28 \pm 0.16 \pm 0.51 \pm 0.03$	2.06 ± 0.06	1.58 ± 0.05
$D_s^+ \rightarrow \pi^0 K^{*+}$	C_{VP}, A	0.75 ± 0.25	$0.51 \pm 0.07 \pm 0.11 \pm 0.01$	0.71 ± 0.03	0.67 ± 0.03
$D_s^+ \rightarrow K^+ \rho^0$	C_{PV}, A	2.17 ± 0.25	$1.84 \pm 0.11 \pm 0.37 \pm 0.18$	1.01 ± 0.03	1.11 ± 0.03
$D_s^+ \rightarrow K^+ \omega$	C_{PV}, A	0.99 ± 0.15	$1.51 \pm 0.09 \pm 0.29 \pm 0.15$	1.66 ± 0.03	1.17 ± 0.03
$D_s^+ \rightarrow K^+ \phi$	T_{VP}, C_{PV}, A	0.18 ± 0.04	$0.24 \pm 0.05 \pm 0.11 \pm 0.03$	0.11 ± 0.01	0.29 ± 0.02
$D_s^+ \rightarrow K^0 \rho^+$	T_{PV}, A	5.46 ± 0.95	$9.35 \pm 0.33 \pm 1.95 \pm 0.94$	7.54 ± 0.27	7.30 ± 0.26
$D_s^+ \rightarrow \eta K^{*+}$	T_{PV}, C_{VP}, A		$1.52 \pm 0.27 \pm 0.52 \pm 0.28$	0.37 ± 0.07	0.39 ± 0.09
$D_s^+ \rightarrow \eta' K^{*+}$	T_{PV}, C_{VP}, A		$0.68 \pm 0.03 \pm 0.16 \pm 0.09$	0.40 ± 0.02	0.42 ± 0.02

TABLE V: Same as Table III for the doubly Cabibbo-suppressed $D \rightarrow PV$ decays in units of 10^{-4} .

Modes	Amplitudes	Br(EXP)	Br(FAT)	Br(F4)	Br(F1')
$D^0 \rightarrow \pi^0 K^{*0}$	C_{PV}, E		$0.95 \pm 0.08 \pm 0.16 \pm 0.10$	0.84 ± 0.04	0.48 ± 0.02
$D^0 \rightarrow \pi^- K^{*+}$	T_{PV}, E	$3.39^{+1.80}_{-1.02}$	$4.91 \pm 0.24 \pm 0.87 \pm 0.49$	3.54 ± 0.28	3.46 ± 0.17
$D^0 \rightarrow K^+ \rho^-$	T_{VP}, E		$1.41 \pm 0.09 \pm 0.35 \pm 0.05$	1.30 ± 0.07	1.32 ± 0.04
$D^0 \rightarrow K^0 \rho^0$	C_{VP}, E		$0.31 \pm 0.04 \pm 0.08 \pm 0.01$	0.25 ± 0.02	0.27 ± 0.01
$D^0 \rightarrow K^0 \omega$	C_{VP}, E		$0.59 \pm 0.05 \pm 0.09 \pm 0.02$	0.66 ± 0.03	0.51 ± 0.02
$D^0 \rightarrow K^0 \phi$	E		$0.18 \pm 0.02 \pm 0.00 \pm 0.03$	0.22 ± 0.01	0.55 ± 0.01
$D^0 \rightarrow \eta K^{*0}$	C_{PV}, E		$0.26 \pm 0.03 \pm 0.05 \pm 0.03$	0.34 ± 0.02	0.20 ± 0.01
$D^0 \rightarrow \eta' K^{*0}$	C_{PV}, E		$0.0037 \pm 0.0005 \pm 0.0004 \pm 0.0004$	0.0019 ± 0.0001	0.0016 ± 0.0001
$D^+ \rightarrow \pi^+ K^{*0}$	C_{PV}, A	3.45 ± 0.6	$3.07 \pm 0.12 \pm 0.68 \pm 0.31$	2.52 ± 0.07	2.51 ± 0.06
$D^+ \rightarrow \pi^0 K^{*+}$	T_{PV}, A	3.4 ± 1.4	$4.54 \pm 0.14 \pm 0.95 \pm 0.45$	4.17 ± 0.15	4.12 ± 0.14
$D^+ \rightarrow K^+ \rho^0$	T_{VP}, A	1.9 ± 0.5	$2.63 \pm 0.10 \pm 0.55 \pm 0.03$	1.84 ± 0.05	1.54 ± 0.04
$D^+ \rightarrow K^+ \omega$	T_{VP}, A	$0.57^{+0.25}_{-0.21}$	$2.10 \pm 0.07 \pm 0.40 \pm 0.03$	2.09 ± 0.05	2.42 ± 0.05
$D^+ \rightarrow K^+ \phi$	A	0.09 ± 0.012	$0.07 \pm 0.01 \pm 0.00 \pm 0.01$	0.057 ± 0.002	0.032 ± 0.003
$D^+ \rightarrow K^0 \rho^+$	C_{VP}, A		$2.17 \pm 0.18 \pm 0.48 \pm 0.04$	1.40 ± 0.06	1.38 ± 0.05
$D^+ \rightarrow \eta K^{*+}$	T_{PV}, A	$4.4^{+1.80}_{-1.50}$	$1.86 \pm 0.08 \pm 0.41 \pm 0.19$	1.44 ± 0.05	1.29 ± 0.04
$D^+ \rightarrow \eta' K^{*+}$	T_{PV}, A		$0.03 \pm 0.00 \pm 0.00 \pm 0.00$	0.016 ± 0.001	0.021 ± 0.001
$D_s^+ \rightarrow K^+ K^{*0}$	T_{VP}, C_{PV}	0.90 ± 0.50	$0.22 \pm 0.02 \pm 0.03 \pm 0.02$	0.20 ± 0.02	0.11 ± 0.02
$D_s^+ \rightarrow K^0 K^{*+}$	T_{PV}, C_{VP}		$1.96 \pm 0.14 \pm 0.67 \pm 0.31$	1.47 ± 0.09	1.44 ± 0.11

decays, $\text{Br}(D^0 \rightarrow \pi^- \rho^+) \approx 2 \text{Br}(D^0 \rightarrow \pi^+ \rho^-)$, $\text{Br}(D^0 \rightarrow K^- K^{*+}) \approx 3 \text{Br}(D^0 \rightarrow K^+ K^{*-})$, $\text{Br}(D^+ \rightarrow \bar{K}^0 K^{*+}) \approx 3 \text{Br}(D^+ \rightarrow K^+ \bar{K}^{*0})$, and $\text{Br}(D_s^+ \rightarrow K^+ \rho^0) \approx 3 \text{Br}(D_s^+ \rightarrow \pi^0 K^{*+})$, and DCS decays, $\text{Br}(D^0 \rightarrow \pi^- K^{*+}) \approx 3 \text{Br}(D^0 \rightarrow K^+ \rho^-)$, $\text{Br}(D^+ \rightarrow \pi^0 K^{*+}) \approx 2 \text{Br}(D^0 \rightarrow K^+ \rho^0)$.

In the FAT approach, the branching ratios of $D_s^+ \rightarrow \pi^+ \rho^0$ and $D_s^+ \rightarrow \pi^0 \rho^+$, which receive contributions solely from A topological diagram, are predicted to be zero. This arises because we do not introduce two distinct parameters χ_P^A and χ_V^A to account for nonfactorizable contributions where the spectator antiquark enters a pseudoscalar (P) or a vector (V) mesons, respectively. Consequently, the contributions from the A diagram involving $u \bar{u}$ forming $\pi^0(\rho^0)$ meson and $d \bar{d}$ forming $\rho^0(\pi^0)$ cancel exactly. As demonstrated in [5], SU(3) symmetry breaking play a more crucial role than the isospin symmetry breaking (which

would be parameterized by χ_P^A and χ_V^A) in D meson decays. We thus employ two parameters, χ_q^A and χ_s^A , to capture SU(3) symmetry breaking effects, rather than introducing additional parameters for subleading isospin symmetry breaking.

D. Direct CP asymmetries

With the fitted parameters in Eq.(11), we calculate the direct CP asymmetries for the $D \rightarrow PV$, as shown in Table VI. The second column in this table lists the penguin topological diagram amplitudes (PT , PC , and PE) in the absence of the tree amplitudes. The direct CP asymmetries in the third column result from the interference between tree and penguin amplitudes. Incorporating contributions from chromomagnetic penguins (cm) and quark loops (ql), which have been absorbed into the penguin Wilson coefficients as specified in Eqs.(5-9), yields the final results presented in the fourth column. The uncertainties in the CP asymmetries originate from the same sources as those in branching ratios, but are now dominated by nonfactorizable parameters due to the significant cancellation of hadronic uncertainties from form factors and decay constants. The updated strong phases in Eq.(11) lead to CP asymmetries that are markedly different from previous results [5]. In contrast to a recent topological diagram approach [9], our results within the FAT approach show significant differences. This discrepancy arises because that study incorporates penguin contributions based on QCD factorization approach, and only the nonfactorizable effects from PE topology are included. Penguin contributions are highly suppressed and consequently cannot interfere effectively with tree amplitudes to generate large CP asymmetries. To date, no CP asymmetries in $D \rightarrow PV$ decays have been definitively measured in experiments. Nevertheless, as shown in Tab.VI, the CP asymmetries in several modes including $D^0 \rightarrow K^0 \bar{K}^{*0}$, $\bar{K}^0 K^{*0}$, $\eta \rho^0$, $\eta' \phi$, $D^+ \rightarrow \pi^+ \rho^0$, $\eta \rho^+$, and $D_s^+ \rightarrow \pi^0 K^{*+}$ are predicted to reach $\mathcal{O}(10^{-3})$, making them promising candidates for future observation at LHCb, Belle II, or BES III. Most CP asymmetries remain at $\mathcal{O}(10^{-5})$, while only a few modes reach $\mathcal{O}(10^{-4})$. For instance, the decays $D^0 \rightarrow \pi^+ \rho^-$, $\pi^- \rho^+$, $K^+ K^{*-}$, and $K^- K^{*+}$ do not attain the same magnitude as their $D \rightarrow PP$ counterparts with the same quark-level transitions, such as $D^0 \rightarrow \pi^+ \pi^-$, and $K^+ K^-$, which are $\mathcal{O}(10^{-4})$ [4]. This difference can be attributed to the distinct strong phases arising from the E and PE topologies in $D \rightarrow PV$ decays compared to those in $D \rightarrow PP$ decays.

TABLE VI: Direct CP asymmetries for the $D \rightarrow PV$ in the units of 10^{-3} . The results from the chromomagnetic penguins and quark loops corrections are also listed in the last column.

Modes	Amplitudes	A_{CP}	$A_{CP}(+cm,ql)$
$D^0 \rightarrow \pi^+ \rho^-$	PT, PE	$-0.04 \pm 0.01 \pm 0.00 \pm 0.00 \quad 0.001 \pm 0.009 \pm 0.003 \pm 0.003$	
$D^0 \rightarrow \pi^0 \rho^0$	PT, PC, PE	$0.01 \pm 0.00 \pm 0.00 \pm 0.00 \quad -0.06 \pm 0.00 \pm 0.00 \pm 0.00$	
$D^0 \rightarrow \pi^0 \omega$	PT, PC, PE	$-0.03 \pm 0.04 \pm 0.02 \pm 0.01 \quad 9.08 \pm 1.43 \pm 1.07 \pm 0.62$	
$D^0 \rightarrow \pi^0 \phi$	PC	$-0.04 \pm 0.01 \pm 0.00 \pm 0.00 \quad -4.21 \pm 0.31 \pm 0.00 \pm 0.00$	
$D^0 \rightarrow \pi^- \rho^+$	PT, PE	$0.03 \pm 0.01 \pm 0.00 \pm 0.00 \quad -0.08 \pm 0.01 \pm 0.00 \pm 0.00$	
$D^0 \rightarrow K^+ K^{*-}$	PT, PE	$0.07 \pm 0.01 \pm 0.01 \pm 0.01 \quad 0.03 \pm 0.01 \pm 0.01 \pm 0.01$	
$D^0 \rightarrow K^0 \bar{K}^{*0}$	PE	$-1.07 \pm 0.16 \pm 0.00 \pm 0.01 \quad -1.07 \pm 0.16 \pm 0.00 \pm 0.01$	
$D^0 \rightarrow \bar{K}^0 K^{*0}$	PE	$-1.07 \pm 0.16 \pm 0.00 \pm 0.01 \quad -1.07 \pm 0.16 \pm 0.00 \pm 0.01$	
$D^0 \rightarrow K^- K^{*+}$	PT, PE	$-0.02 \pm 0.01 \pm 0.00 \pm 0.00 \quad 0.15 \pm 0.01 \pm 0.00 \pm 0.00$	
$D^0 \rightarrow \eta \rho^0$	$PT, PC, PE,$	$1.02 \pm 0.13 \pm 0.09 \pm 0.04 \quad 1.06 \pm 0.15 \pm 0.08 \pm 0.04$	
$D^0 \rightarrow \eta \omega$	PT, PC, PE	$-0.16 \pm 0.03 \pm 0.00 \pm 0.00 \quad 1.68 \pm 0.09 \pm 0.18 \pm 0.06$	
$D^0 \rightarrow \eta \phi$	PC, PE	$-0.04 \pm 0.00 \pm 0.01 \pm 0.01 \quad -1.00 \pm 0.43 \pm 0.74 \pm 0.36$	
$D^0 \rightarrow \eta' \rho^0$	PT, PC, PE	$-0.02 \pm 0.03 \pm 0.00 \pm 0.00 \quad 0.29 \pm 0.06 \pm 0.04 \pm 0.01$	
$D^0 \rightarrow \eta' \omega$	PT, PC, PE	$0.29 \pm 0.23 \pm 0.02 \pm 0.01 \quad 5.37 \pm 0.56 \pm 0.58 \pm 0.19$	
$D^0 \rightarrow \eta' \phi$	PT, PC, PE	$-0.85 \pm 0.82 \pm 0.06 \pm 0.01 \quad -4.45 \pm 2.36 \pm 0.01 \pm 0.04$	
$D^+ \rightarrow \pi^+ \rho^0$	PT, PC	$-1.65 \pm 0.12 \pm 0.46 \pm 0.16 \quad -1.35 \pm 0.11 \pm 0.63 \pm 0.22$	
$D^+ \rightarrow \pi^+ \omega$	PT, PC	$0.32 \pm 0.07 \pm 0.30 \pm 0.10 \quad -10.32 \pm 2.60 \pm 0.58 \pm 0.43$	
$D^+ \rightarrow \pi^+ \phi$	PC	$-0.04 \pm 0.01 \pm 0.00 \pm 0.00 \quad -4.15 \pm 0.31 \pm 0.00 \pm 0.00$	
$D^+ \rightarrow \pi^0 \rho^+$	PT, PC	$-0.15 \pm 0.04 \pm 0.06 \pm 0.02 \quad -0.40 \pm 0.04 \pm 0.09 \pm 0.03$	
$D^+ \rightarrow K^+ \bar{K}^{*0}$	PT	$0.25 \pm 0.05 \pm 0.04 \pm 0.02 \quad 0.21 \pm 0.05 \pm 0.03 \pm 0.02$	
$D^+ \rightarrow \bar{K}^0 K^{*+}$	PT	$0.08 \pm 0.02 \pm 0.01 \pm 0.00 \quad 0.24 \pm 0.02 \pm 0.01 \pm 0.01$	
$D^+ \rightarrow \eta \rho^+$	PT, PC	$4.00 \pm 1.31 \pm 2.76 \pm 1.06 \quad 4.11 \pm 1.50 \pm 2.42 \pm 0.94$	
$D^+ \rightarrow \eta' \rho^+$	PT, PC	$-0.04 \pm 0.01 \pm 0.01 \pm 0.00 \quad 0.28 \pm 0.03 \pm 0.03 \pm 0.01$	
$D_s^+ \rightarrow \pi^+ K^{*0}$	PT	$-0.22 \pm 0.04 \pm 0.03 \pm 0.02 \quad -0.17 \pm 0.05 \pm 0.03 \pm 0.02$	
$D_s^+ \rightarrow \pi^0 K^{*+}$	PT, PC	$-0.58 \pm 0.06 \pm 0.05 \pm 0.04 \quad -0.52 \pm 0.06 \pm 0.05 \pm 0.04$	
$D_s^+ \rightarrow K^+ \rho^0$	PT, PC	$0.07 \pm 0.01 \pm 0.02 \pm 0.01 \quad -0.08 \pm 0.01 \pm 0.02 \pm 0.01$	
$D_s^+ \rightarrow K^+ \omega$	PT, PC	$-0.13 \pm 0.02 \pm 0.02 \pm 0.01 \quad 5.06 \pm 0.24 \pm 0.06 \pm 0.03$	
$D_s^+ \rightarrow K^+ \phi$	PT, PC	$0.28 \pm 0.04 \pm 0.13 \pm 0.04 \quad 3.40 \pm 1.00 \pm 3.92 \pm 1.23$	
$D_s^+ \rightarrow K^0 \rho^+$	PT	$0.10 \pm 0.01 \pm 0.01 \pm 0.01 \quad -0.01 \pm 0.01 \pm 0.01 \pm 0.01$	
$D_s^+ \rightarrow \eta K^{*+}$	PT, PC	$-0.16 \pm 0.02 \pm 0.06 \pm 0.02 \quad 0.03 \pm 0.05 \pm 0.06 \pm 0.02$	
$D_s^+ \rightarrow \eta' K^{*+}$	PT, PC	$-0.06 \pm 0.02 \pm 0.02 \pm 0.01 \quad -0.15 \pm 0.02 \pm 0.05 \pm 0.02$	

The corrections from the chromomagnetic penguins and quark loops are substantial, as they can significantly change the size or even flip the signs of CP asymmetries. A notable example is found in the decays $D^0 \rightarrow \pi^0\phi$ and $D^+ \rightarrow \pi^+\phi$, where asymmetries involving C_{PV} and PC_{PV} topologies are enhanced from $\mathcal{O}(10^{-5})$ to $\mathcal{O}(10^{-3})$. This enhancement occurs because the chromomagnetic penguins and quark loops corrections to $C_{4,6}$ increase the magnitude of PC_{PV} amplitude, thereby strengthening its interference with the C_{PV} amplitude. Consequently, precise measurements of CP asymmetries are crucial in the search for new physics, which could manifest through modifications to the penguin Wilson coefficients similar to those induced by the chromomagnetic penguins and quark loops corrections within the Standard Model.

IV. CONCLUSION

Driven by extensive new measurements and improved precision of charm decays, we present an updated analysis of two-body $D \rightarrow PV$ decays under the framework of FAT. The nonfactorizable contributions to all $D \rightarrow PV$ decay amplitudes are described by only 15 universal parameters after factoring out form factors and decay constants, capturing flavor $SU(3)$ breaking effects. In contrast to earlier FAT analyses, we introduce an additional nonfactorizable parameter χ^T for the T diagram, which we find to be non-negligible given current high-precision data even in the so-called “factorizable T diagram. All parameters including χ^T , the nonfactorizable topological amplitudes, $\chi_{V(P)}^C$, $\chi_{q(s)}^E$, $\chi_{q(s)}^A$, their associated strong phase $\phi_{V(P)}^C$, $\phi_{q(s)}^E$, $\phi_{q(s)}^A$, the Glauber phase S_π , and the soft scale Λ_{QCD} , are fitted globally from 41 $D \rightarrow PV$ branching ratios measurements. Although the T topology remains dominant, the C topology also exhibits substantial nonfactorizable effects. The parameters χ_P^C and χ_V^C for the C amplitude show only minor deviations from earlier FAT studies. More pronounced discrepancies are observed in the subleading power E and A topologies, which are governed by nonfactorizable dynamics. These small values of $\chi_{q,s}^{E,A}$ together with their strong phases $\phi_{q,s}^{E,A}$ and the Glauber phase S_π highlight the need for more high-precision data to properly constrain these contributions.

Using the updated nonfactorizable parameters, we predict $D \rightarrow PV$ branching ratios with improved precision, yielding results consistent with current experimental data and the latest results in topological diagram approach. We also calculate the direct CP asymmetries arising

from interference between tree and penguin diagrams. Owing to the substantial updates in the determined strong phases, our CP asymmetry predictions differ notably from earlier FAT values. Several CP asymmetries are predicted to as large as $\mathcal{O}(10^{-3})$, rendering them promising observables for future high-precision experiments. Predictions are also provided for unobserved decay modes, particularly those with branching fractions in the $10^{-4} - 10^{-3}$ range, offering key target for upcoming experimental studies.

Acknowledgments

We are grateful to Qin Qin for useful discussions. The work is supported by the National Natural Science Foundation of China under Grants No.12465017 and No.12105148.

- [1] H.-Y. Cheng and C.-W. Chiang, *Two-body hadronic charmed meson decays*, *Phys. Rev. D* **81** (2010) 074021, [[arXiv:1001.0987](https://arxiv.org/abs/1001.0987)].
- [2] B. Bhattacharya and J. L. Rosner, *Charmed meson decays to two pseudoscalars*, *Phys. Rev. D* **81** (2010) 014026, [[arXiv:0911.2812](https://arxiv.org/abs/0911.2812)].
- [3] H.-Y. Cheng and C.-W. Chiang, *Direct CP violation in two-body hadronic charmed meson decays*, *Phys. Rev. D* **85** (2012) 034036, [[arXiv:1201.0785](https://arxiv.org/abs/1201.0785)]. [Erratum: *Phys. Rev. D* 85, 079903 (2012)].
- [4] H.-n. Li, C.-D. Lu, and F.-S. Yu, *Branching ratios and direct CP asymmetries in $D \rightarrow PP$ decays*, *Phys. Rev. D* **86** (2012) 036012, [[arXiv:1203.3120](https://arxiv.org/abs/1203.3120)].
- [5] Q. Qin, H.-n. Li, C.-D. Lü, and F.-S. Yu, *Branching ratios and direct CP asymmetries in $D \rightarrow PV$ decays*, *Phys. Rev. D* **89** (2014), no. 5 054006, [[arXiv:1305.7021](https://arxiv.org/abs/1305.7021)].
- [6] **LHCb** Collaboration, R. Aaij et al., *Observation of CP Violation in Charm Decays*, *Phys. Rev. Lett.* **122** (2019), no. 21 211803, [[arXiv:1903.08726](https://arxiv.org/abs/1903.08726)].
- [7] H.-Y. Cheng, C.-W. Chiang, and A.-L. Kuo, *Global analysis of two-body $D \rightarrow VP$ decays within the framework of flavor symmetry*, *Phys. Rev. D* **93** (2016), no. 11 114010, [[arXiv:1604.03761](https://arxiv.org/abs/1604.03761)].
- [8] H.-Y. Cheng and C.-W. Chiang, *Revisiting CP violation in $D \rightarrow PP$ and VP decays*, *Phys. Rev. D* **100** (2019), no. 9 093002, [[arXiv:1909.03063](https://arxiv.org/abs/1909.03063)].

[9] H.-Y. Cheng and C.-W. Chiang, *CP violation in quasi-two-body $D \rightarrow VP$ decays and three-body D decays mediated by vector resonances*, *Phys. Rev. D* **104** (2021), no. 7 073003, [[arXiv:2104.13548](https://arxiv.org/abs/2104.13548)].

[10] H.-Y. Cheng and C.-W. Chiang, *Updated analysis of $D \rightarrow PP, VP$, and VV decays: Implications for $KS0-KL0$ asymmetries and $D0-D^-0$ mixing*, *Phys. Rev. D* **109** (2024), no. 7 073008, [[arXiv:2401.06316](https://arxiv.org/abs/2401.06316)].

[11] S.-H. Zhou, Y.-B. Wei, Q. Qin, Y. Li, F.-S. Yu, and C.-D. Lu, *Analysis of Two-body Charmed B Meson Decays in Factorization-Assisted Topological-Amplitude Approach*, *Phys. Rev. D* **92** (2015), no. 9 094016, [[arXiv:1509.04060](https://arxiv.org/abs/1509.04060)].

[12] S.-H. Zhou, Q.-A. Zhang, W.-R. Lyu, and C.-D. Lü, *Analysis of Charmless Two-body B decays in Factorization Assisted Topological Amplitude Approach*, *Eur. Phys. J. C* **77** (2017), no. 2 125, [[arXiv:1608.02819](https://arxiv.org/abs/1608.02819)].

[13] C. Wang, Q.-A. Zhang, Y. Li, and C.-D. Lu, *Charmless $B_{(s)} \rightarrow VV$ Decays in Factorization-Assisted Topological-Amplitude Approach*, *Eur. Phys. J. C* **77** (2017), no. 5 333, [[arXiv:1701.01300](https://arxiv.org/abs/1701.01300)].

[14] H.-Y. Jiang, F.-S. Yu, Q. Qin, H.-n. Li, and C.-D. Lü, *D^0 - \bar{D}^0 mixing parameter y in the factorization-assisted topological-amplitude approach*, *Chin. Phys. C* **42** (2018), no. 6 063101, [[arXiv:1705.07335](https://arxiv.org/abs/1705.07335)].

[15] D. Wang, F.-S. Yu, P.-F. Guo, and H.-Y. Jiang, *$K_S^0 - K_L^0$ asymmetries in D -meson decays*, *Phys. Rev. D* **95** (2017), no. 7 073007, [[arXiv:1701.07173](https://arxiv.org/abs/1701.07173)].

[16] F.-S. Yu, D. Wang, and H.-n. Li, *CP asymmetries in charm decays into neutral kaons*, *Phys. Rev. Lett.* **119** (2017), no. 18 181802, [[arXiv:1707.09297](https://arxiv.org/abs/1707.09297)].

[17] S.-H. Zhou and C.-D. Lü, *Extraction of the CKM phase γ from the charmless two-body B meson decays*, *Chin. Phys. C* **44** (2020), no. 6 063101, [[arXiv:1910.03160](https://arxiv.org/abs/1910.03160)].

[18] Q. Qin, C. Wang, D. Wang, and S.-H. Zhou, *The factorization-assisted topological-amplitude approach and its applications*, *Front. Phys. (Beijing)* **18** (2023), no. 6 64602, [[arXiv:2111.14472](https://arxiv.org/abs/2111.14472)].

[19] S.-H. Zhou, R.-H. Li, Z.-Y. Wei, and C.-D. Lu, *Analysis of three-body charmed B -meson decays under the factorization-assisted topological-amplitude approach*, *Phys. Rev. D* **104** (2021), no. 11 116012, [[arXiv:2107.11079](https://arxiv.org/abs/2107.11079)].

[20] S.-H. Zhou, X.-X. Hai, R.-H. Li, and C.-D. Lu, *Analysis of three-body charmless B -meson*

decays under the factorization-assisted topological-amplitude approach, *Phys. Rev. D* **107** (2023), no. 11 116023, [[arXiv:2305.02811](https://arxiv.org/abs/2305.02811)].

[21] S.-H. Zhou, R.-H. Li, and X.-Y. Lü, *Analysis of three-body decays $B \rightarrow D(V \rightarrow)PP$ under the factorization-assisted topological-amplitude approach*, *Phys. Rev. D* **110** (2024), no. 5 056001, [[arXiv:2406.00373](https://arxiv.org/abs/2406.00373)].

[22] J. Ou-Yang, R.-H. Li, and S.-H. Zhou, *Analysis of three-body charmed B meson decays $B \rightarrow D(V^* \rightarrow)VP$* , *Phys. Rev. D* **112** (2025), no. 5 056005, [[arXiv:2506.14675](https://arxiv.org/abs/2506.14675)].

[23] X.-D. Zhou and S.-H. Zhou, *Analysis of three-body hadronic D -meson decays*, *Phys. Rev. D* **111** (2025), no. 11 116008, [[arXiv:2503.18593](https://arxiv.org/abs/2503.18593)].

[24] W.-F. Wang, J.-Y. Xu, S.-H. Zhou, and P.-P. Shi, *Contributions of $\rho(770, 1450) \rightarrow \omega\pi$ for the Cabibbo-favored $D \rightarrow h\omega\pi$ decays*, [[arXiv:2502.11159](https://arxiv.org/abs/2502.11159)].

[25] Z.-T. Zou, C. Li, and C.-D. Lü, *Pure annihilation type $D \rightarrow PP(V)$ decays in the perturbative QCD approach*, *Chin. Phys. C* **37** (2013) 093101, [[arXiv:1301.3444](https://arxiv.org/abs/1301.3444)].

[26] M. Beneke, G. Buchalla, M. Neubert, and C. T. Sachrajda, *QCD factorization for $B \rightarrow \pi\pi$ decays: Strong phases and CP violation in the heavy quark limit*, *Phys. Rev. Lett.* **83** (1999) 1914–1917, [[hep-ph/9905312](https://arxiv.org/abs/hep-ph/9905312)].

[27] M. Beneke, G. Buchalla, M. Neubert, and C. T. Sachrajda, *QCD factorization for exclusive, nonleptonic B meson decays: General arguments and the case of heavy light final states*, *Nucl. Phys. B* **591** (2000) 313–418, [[hep-ph/0006124](https://arxiv.org/abs/hep-ph/0006124)].

[28] M. Beneke and M. Neubert, *QCD factorization for $B \rightarrow PP$ and $B \rightarrow PV$ decays*, *Nucl. Phys. B* **675** (2003) 333–415, [[hep-ph/0308039](https://arxiv.org/abs/hep-ph/0308039)].

[29] **Particle Data Group** Collaboration, S. Navas et al., *Review of particle physics*, *Phys. Rev. D* **110** (2024), no. 3 030001.

[30] **CLEO** Collaboration, D. Besson et al., *Improved measurements of D meson semileptonic decays to π and K mesons*, *Phys. Rev. D* **80** (2009) 032005, [[arXiv:0906.2983](https://arxiv.org/abs/0906.2983)].

[31] **Belle** Collaboration, L. Widhalm et al., *Measurement of $D^0 \rightarrow \pi\ell\nu(K\ell\nu)$ Form Factors and Absolute Branching Fractions*, *Phys. Rev. Lett.* **97** (2006) 061804, [[hep-ex/0604049](https://arxiv.org/abs/hep-ex/0604049)].

[32] **BESIII** Collaboration, M. Ablikim et al., *First Measurement of the Form Factors in $D_s^+ \rightarrow K^0 e^+ \nu_e$ and $D_s^+ \rightarrow K^{*0} e^+ \nu_e$ Decays*, *Phys. Rev. Lett.* **122** (2019), no. 6 061801, [[arXiv:1811.02911](https://arxiv.org/abs/1811.02911)].

[33] **BESIII** Collaboration, M. Ablikim et al., *Improved measurement of the semileptonic decay*

$D_s^+ \rightarrow K^0 e^+ \nu_e$, [Phys. Rev. D](#) **110** (2024), no. 5 052012, [[arXiv:2406.19190](#)].

[34] C. Bernard et al., *Visualization of semileptonic form factors from lattice QCD*, [Phys. Rev. D](#) **80** (2009) 034026, [[arXiv:0906.2498](#)].

[35] D.-S. Du, J.-W. Li, and M.-Z. Yang, *Form-factors and semileptonic decay of $D_s^+ \rightarrow \phi \bar{l} \nu$ from QCD sum rule*, [Eur. Phys. J. C](#) **37** (2004), no. 2 173–184, [[hep-ph/0308259](#)].

[36] H.-J. Tian, Y.-L. Yang, D.-D. Hu, H.-B. Fu, T. Zhong, and X.-G. Wu, *Searching for $|V_{cd}|$ through the exclusive decay $D_s^+ \rightarrow K^0 e^+ \nu_e$ within QCD sum rules*, [Phys. Lett. B](#) **857** (2024) 138975, [[arXiv:2405.07154](#)].

[37] D. Melikhov and B. Stech, *Weak form-factors for heavy meson decays: An Update*, [Phys. Rev. D](#) **62** (2000) 014006, [[hep-ph/0001113](#)].

[38] C.-H. Chen, Y.-L. Shen, and W. Wang, $|V_{ub}|$ and $B \rightarrow \eta^{(\prime)}$ Form Factors in Covariant Light Front Approach, [Phys. Lett. B](#) **686** (2010) 118–123, [[arXiv:0911.2875](#)].

[39] R. C. Verma, *Decay constants and form factors of s-wave and p-wave mesons in the covariant light-front quark model*, [J. Phys. G](#) **39** (2012) 025005, [[arXiv:1103.2973](#)].

[40] W. Wang and Y.-L. Shen, $D_s \rightarrow K, K^*$, phi form factors in the Covariant Light-Front Approach and Exclusive D_s Decays, [Phys. Rev. D](#) **78** (2008) 054002.

[41] D.-D. Hu, X.-G. Wu, L. Zeng, H.-B. Fu, and T. Zhong, *Improved light-cone harmonic oscillator model for the ϕ -meson longitudinal leading-twist light-cone distribution amplitude and its effects to $D_s^+ \rightarrow \phi \ell^+ \nu_\ell$* , [Phys. Rev. D](#) **110** (2024), no. 5 056017, [[arXiv:2403.10003](#)].

[42] S. Fajfer and J. F. Kamenik, *Charm meson resonances and $D \rightarrow V$ semileptonic form-factors*, [Phys. Rev. D](#) **72** (2005) 034029, [[hep-ph/0506051](#)].

[43] S. Momeni and M. Saghebfar, *Semileptonic D meson decays to the vector, axial vector and scalar mesons in Hard-Wall AdS/QCD correspondence*, [Eur. Phys. J. C](#) **82** (2022), no. 5 473.

[44] H. A. Ahmed, Y. Chen, and M. Huang, *$D_{(s)}$ -mesons semileptonic form factors in four-flavor holographic QCD*, [Phys. Rev. D](#) **109** (2024), no. 2 026008, [[arXiv:2309.06156](#)].

[45] Y. Fu-Sheng, X.-X. Wang, and C.-D. Lu, *Nonleptonic Two Body Decays of Charmed Mesons*, [Phys. Rev. D](#) **84** (2011) 074019, [[arXiv:1101.4714](#)].